Scientific paper

Synthesis, Crystal Structure, Hirshfeld Surface Analysis, and DFT Calculations of the New Binuclear Copper(I) Complex Containing 2-Benzimidazolethiole and Triphenylphosphine Ligands

Karwan Omer Ali

Department of General Science, College of Education, University of Halabja, Halabja 46018, Iraq

** Corresponding author: E-mail: karwan.ali@uoh.edu.iq*
Phone No. 009647503849284

Received: 08-26-2023

Abstract

The reaction of 2-benzimidazolethiole (L) with copper dichloride in the presence of two equivalents of triphenylphosphine led to a binuclear complex of the type $[Cu(L)_2(Ph_3P)_2Cl_2]$: dichloridobis(μ-1,3-dihydro-2H-benzimidazole-2-thione) bis(triphenylphosphine)-di-copper. The Cu(I) compound has been fully identified by elemental analysis, molar conductivity, FT-IR, UV/Vis, and single-crystal X-ray diffraction (XRD). The XRD study reveals that the complex has distorted tetrahedral geometry around the Cu(I) center, which contains two bridge sulfur atoms. The Hirshfeld surface mapped over d_{norm}, shape index, and curvature revealed important H···H, H···C/C···H, and H···Cl/Cl···H intermolecular interactions as the main contributors to crystal packing. The natural bond orbital (NBO) was applied to understand the strength of nucleophilic and electrophilic attack between ligands and Cu(I) ions. Furthermore, density functional theory (DFT) was employed to demonstrate the molecular reactivity and stability of the ligands and copper complex.

Keywords: Copper(I), 2-benzimidazolethiole, distorted tetrahedral geometry, Hirshfeld surface analysis, DFT studies

1. Introduction

The extensive study currently conducted in Cu(I) coordination compounds is due to the interactions of this cation in particular chemical redox reactions and can utilize a variety of coordination modes.[1] Cu(I) halides produce complexes with triphenylphosphine as ligands that have copper halide to ligand ratios of 1:2, 2:2, 1:3, 2:3, and 2:4 with the geometry typically being controlled by steric instead of electronic properties of the phosphine ligands.[2,3] Due to their lower toxicity, greater availability, and comparably lower cost compared to third-row transition metal compounds including rhenium, iridium, platinum, and gold, Cu(I) complexes with irregular square planar and tetrahedral geometry are in perpetual interest.[4] For a long time, there is a continuous interest about chelating agents comprising nitrogen and sulfur-donor atoms among with their metal complexes.[5,6] This consideration results from their antimicrobial,[7] antitumour[8,9] activities along with other numerous potential pharmaceutical applications.[10] Several mixed-ligand coordination complexes of Cu(I) halides with thione compounds and triphenylphosphines were synthesized and structurally determined during our previous study on the interaction of univalent group IB metals with biologically important molecules.[11,12] In such complexes, neutral thione ligands that contained both nitrogen and sulfur as donor atoms regularly adopted the unidentate coordination mode, coordinating with the metal ions via the exocyclic sulfur atom in a bridging or terminal form .[13] However, an incredible variety of complexes, ranging from mononuclear three- or four-coordinate thiones with square planar and tetrahedral Cu(I), respectively, to dimers with distorted tetrahedral geometry, are produced by bridging thione ligands through sulfur atoms.[14,15] For decades, mixed-ligand complexes have pinched a lot of attention as a result of their serious function in biological processes. Numerous studies[16–22] have discussed the production and spectral investigation of mixed-ligand complexes. It was found that the insertion of heterocyclic nitrogen donor ligands, such as nitrogen, oxygen-donors like 8-hydroxyquinoline or nitrogen, nitrogen-donors like 1,10-phenanthroline, significantly en-

hanced the biological and pharmacological actions of the complexes.[16–23] In the current study, a new Cu(I) complex based on a 2-benzimidazolethiole ligand (L) was synthesized and investigated. This complex was characterized using elemental analysis, molar conductivity, FT-IR, UV-Vis, and X-ray analysis. Hirshfeld surface analysis was also used to confirm the crystal structure, which is useful for interpreting the intermolecular forces in crystal packing. DFT simulations were also carried out to forecast the complex's electronic and geometrical structure.

2. Experimental

2. 1. Materials and General Methods

In this study, methanol (99%), dichloromethane (99.7%), and dimethyl sulfoxide (99.8%) were bought from Alfa Aesar and used without further purification. The Sigma-Aldrich product 2-benzimidazolethiole (L) was used directly. At 296 K, a Bruker Kappa Apex II diffractometer was used to measure the single-crystal X-ray structure with a radiation wavelength of (λ = 0.71073). The EURO EA 300 CHNS analyzer was used to determine the percentages of C, H, N, and S. Infrared spectra in the 4000–400 cm^{-1} and 600–200 cm^{-1} range as KBr and CsI discs, respectively, were taken using a Shimadzu FT-IR-8400S spectrophotometer. On the AEUV1609 LTD Shimadzu spectrophotometer, the UV-visible spectra of the compounds in DMSO were measured. On a Meter CON 700 Benchtop Conductivity Meter, the molar conductivities of 10^{-3} M solutions of the complex and ligands in DMSO were measured at 25 °C. The Scientific Stuart SMP3 melting point apparatus was used to determine the melting point of the complex.

2. 2. Synthesis of $[Cu(L)_2(Ph_3P)_2Cl_2]$

Dropwise under stirring, a solution of $CuCl_2.H_2O$ (0.341 g, 2.0 mmol) in methanol (20 mL) was added to a solution mixture of 2-benzimidazolethiole (L) ligand (0.300 g, 2.0 mmol) and triphenylphosphine ligand (0.524 g, 2.0 mmol) in dichloromethane (25 mL). After that, the mixture was stirred for 4 h. at room temperature, resulting in the formation of a clear solution, which was then slowly evaporated at room temperature to produce white crystalline products within two weeks. m.p. 238–239 °C. Yield: 0.947 g (81.60 %). Anal. Calcd. for $C_{50}H_{42}Cl_2Cu_2N_4P_2S_2$: C 58.65, H 4.10, N 5.47, S 6.25. Found: C 58.58, H 4.12, N 5.48, S 6.22. Molar conductivity: 7.31×10^{-5} S cm^2 mol^{-1}. FT-IR (KBr) 3138, 3097, 3055, 1620, 1508, 1458, 1348, 734, 697, 457 cm^{-1}. UV-Vis data in DMSO [λ/nm, (cm^{-1})]: 316(31645), 247(40485).

2. 3. X-ray Crystal Structure Determination

A Bruker Kappa Apex II X-ray diffractometer with graphite monochromated Mo-Ka radiation (λ = 0.71073) at 296 K was used to measure the X-ray diffraction of the Cu(I) complex. The crystallographic software SHELXT-2018 was used to solve the structure using a dual-space algorithm, and SHELXL-2018/3 was used to refine it using least-squares procedures. All C, N, Cl, S, and Cu atoms were anisotropically resolved.[24,25] All of the C, N, Cl, S, and Cu atoms were resolved anisotropically. The hydrogen atoms bound to the C atoms were permitted to rotate geometrically and were treated as a riding model with a C-H distance of 0.93 Å (aromatic), 1.72 Å (C-S group), and 0.84 Å (-NH group).[26] The complex's crystal data and structure refinement details have been collected in Table 1.

Table 1. Crystal data and structure refinement of the complex

Formula	$C_{50}H_{42}Cl_2Cu_2N_4P_2S_2$
Formula weight	1022.94
Temperature, K	296
Wavelength, Å	0.71073
Crystal system	triclinic
Space group	P-1 (No. 2)
Crystal size, mm	0.18 x 0.43 x 0.47
a / Å	12.4699(7)
b / Å	13.7519(7)
c / Å	14.0572(6)
α / °	95.051(2)
β / °	91.866(2)
γ / °	103.818(2)
V / Å^3	2328.2(2)
Z	2
D_c / g cm^{-3}	1.459
μ(Mo-Kα) (mm^{-1})	1.227
θ range for data collection, °	1.5,28.4
Dataset	–16:16; –18:18; –18:18
F 000	1048
No. of reflections	11605
No. of parameters	575
R_{int}	0.022
R_1, wR_2	0.0320, 0.0855
S	1.04
[$I > 2\sigma(I)$]	9718
$\Delta\rho_{min}$, $\Delta\rho_{max}$ / eÅ^{-3}	–1.08, 1.02

2. 4. Computational Details

Density functional theory (DFT) calculations were performed using the Gaussian 09 software program to better understand the structure of the copper complex. The Gauss View 6.0 program at the B3LYP level of theory was helpful in determining the frontier molecular orbitals of the ligand and the Cu(I) complex.[27] In particular, the 6-31G(d) basis set for non-metal elements (C, H, N, S, and Cl) and the LANL2DZ basis set for the copper metal atom were both studied.[28] Using the same level of theory, the complex's neutral bond orbital (NBO) analysis was carried out using the Gaussian 06 program.[29]

2. 5. Hirshfeld Surface

For the Hirshfeld surface visualization of the Cu(I) complex, a crystallographic information file (CIF) obtained from single-crystal X-ray diffraction studies used as the input file. Using the program Crystal Explorer 21.5, the Hirshfeld surface analysis was generated in order to better understand the intermolecular interactions in the complex crystal structure.[30] Using the same program, 2D fingerprint plots with dean d_e and d_i distances were calculated, Hirshfeld surface visualization was performed, and results were presented as d_{norm}, shape index, and curvedness.[31]

3. Results and Discussion

The 2-benzimidazolethiole (L) and triphenylphosphine ligands react with Cu(II) chloride to produce the Cu(I) complex, as illustrated in Scheme 1. In this reaction, Cu(II) is reduced to Cu(I) by triphenylphosphine, which acts as a reducing agent. Under atmospheric conditions, the synthesized Cu(I) compound complex is stable. The metal complex was successfully synthesized as white crystals with a good yield suitable for single-crystal X-ray structure analysis. The complex dissolves in common organic solvents such dimethyl sulfoxide, dimethylformamide, and chloroform at ambient temperature but not in ethanol, acetone, methanol, or water.

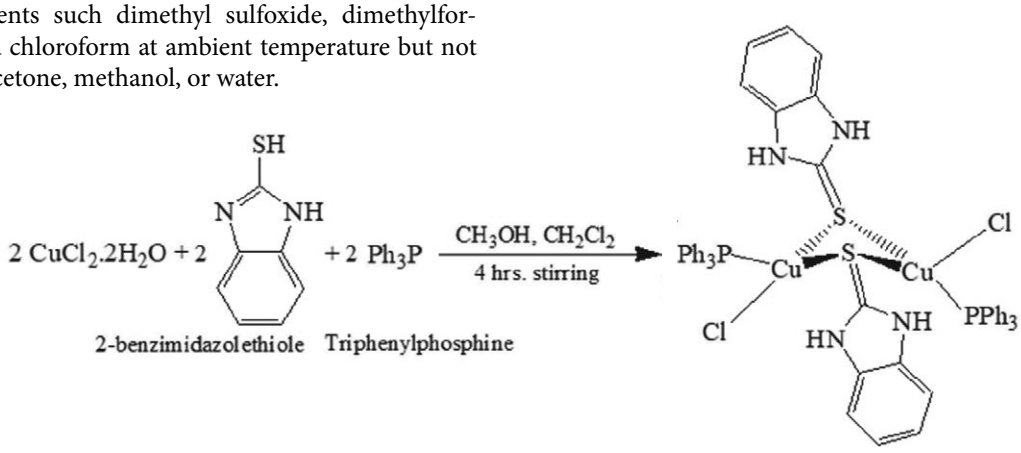

Scheme 1. Synthetic route of the Cu(I) complex.

3. 1. Description of the Cu(I) Crystal Structure

The main bond lengths and angles for the Cu(I) complex are given in Table 2, and Table 3 shows the details of the hydrogen bonding. Figure 1 display molecular plots that display the atom numbering schemes. The two copper atoms are surrounded by one P and one Cl atom in a distorted tetrahedral coordination, producing a binuclear complex. The two copper atoms are bridged by two sulfur atoms. The largest variation from the ideal tetrahedral geometry is reflected by the Cl1-Cu1-S1, Cl1-Cu1-P2, S1-Cu1-P2, and Cl2-Cu2-S3 bond angles, with values of 113.40(2), 114.65(2), 116.40(2), and 112.67(2), respectively. These higher bond angles are counterbalanced by the bond angles Cu1-S1-Cu1_a and Cu2-S3-Cu2_b, whose values are all less than the ideal tetrahedral value of 109.5°. The bulky triphenylphosphine and the 2-benzimidazolethiole (L) ligands often interact sterically to cause this tetrahedral distortion in a large number of dimeric copper (I) complexes that also contain one heterocyclic thione and two monodentate triphenylphosphine ligands.[32] The bond lengths between Cu1-P2 (2.2379(5)) and Cu2-P4 (2.2371(5)) are shorter than those between Cu1-S1 (2.3256(6)) and Cu2-S3 (2.3580(5)), showing that the interaction between Cu(I) metal center and P donor atom is stronger than that between Cu(I) and S donor atom. The torsional angles of Cl1-Cu1-S1-Cu1_a, P2-Cu1-S1-C17, and Cl1-Cu1-P2-C211 are 100.94(2)°, 130.32(7)°, and 179.75(7)°, respectively, which results in steric repulsion between triphenylphosphine and thione rings and electron repulsion of chlorine and nitrogen atoms.[33] In the crystal structure of the Cu(I) complex, there are intermolecular N11–H11…Cl1, N12–H12…Cl2, N31–H31…Cl2, N32–H32…Cl1, C212–H212…N11 and C433–H433…Cl1 hydrogen bonds, the nitrogen and carbon atoms of the ligand acts as proton donors, whereas the chlorine acts as proton acceptors.

Table 2. Selected bond lengths (Å) and angles (°) of the complex.

Bond	Distances, Å	Bond	Angle, °
Cu1-Cl1	2.3402(5)	Cl1-Cu1-S1	113.40(2)
Cu1-S1	2.3256(6)	Cl1-Cu1-P2	114.65(2)
Cu1-P2	2.2379(5)	Cl1-Cu1-S1_a	93.49(2)
Cu1-S1_a	2.6203(6)	S1-Cu1-P2	116.40(2)
Cu2-Cl2	2.3563(7)	S1-Cu1-S1_a	105.63(2)
Cu2-S3	2.3580(5)	S1_a -Cu1-P2	110.35(2)
Cu2-P4	2.2371(5)	S3-Cu2-S3_b	103.82(2)
Cu2-S3_b	2.4727(5)	S3_b-Cu2-P4	114.30(2)
S1-C17	1.7094(19)	Cl2-Cu2-S3	112.67(2)
P2-C211	1.8237(18)	Cl2-Cu2-P4	107.02(2)
P2-C221	1.8236(19)	Cl2-Cu2-S3_b	101.37(2)
P2-C231	1.822(2)	Cu1-S1-Cu1_a	74.37(2)
S3-C37	1.721(2)	Cu2-S3-Cu2_b	76.18(2)

Table 3. Hydrogen bonding (Å, °) for Cu(I) complex.

D–H···A	*d*(D–H) / Å	*d*(H···A) / Å	*d*(D···A) / Å	<(DHA) / °
N11–H11···Cl1	0.84(2)	2.28(2)	3.1076(17)	166(2)
N12–H12···Cl2	0.840(18)	2.52(2)	3.2323(18)	143(2)
N31–H31···Cl2	0.86(2)	2.24(2)	3.0648(19)	159(2)
N32–H32···Cl1	0.855(19)	2.376(19)	3.2021(19)	163(2)
C212–H212···N11	0.9300	2.5300	3.255(3)	135.00
C433–H433···Cl1	0.9300	2.8200	3.548(3)	136.00

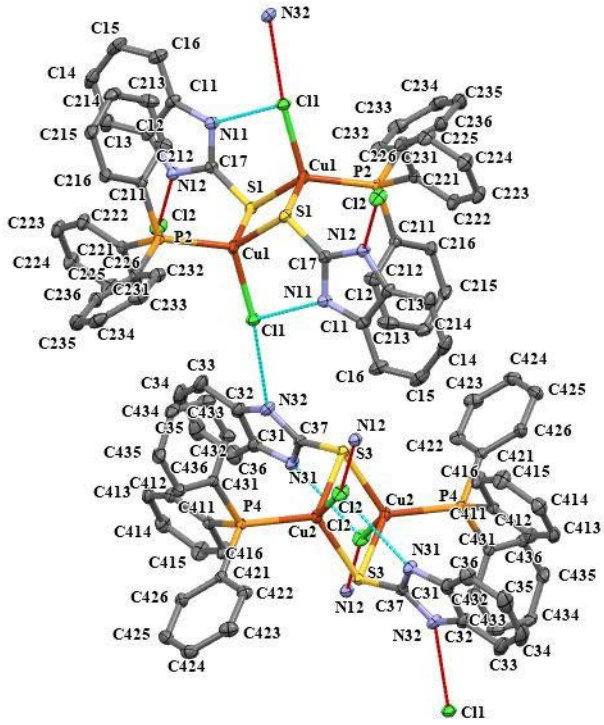

Figure 1. Crystal structure of $[Cu(\mu\text{-S-2-BIT})_2(Ph_3P)_2Cl_2]$ shown at 20% ellipsoid probability, H atoms are omitted for clarity.

3. 2. FT-IR Spectra

The medium intensity peak at 3155 cm^{-1} in the IR spectrum of the ligand (2-BIT) can be attributed to the stretching vibration of the NH group, which is shifted by 17 cm^{-1} to a lower frequency due to hydrogen bonding because hydrogen bonding weakens the N-H bond, resulting in its absorption frequency being lower.[34] The infrared spectrum of the Cu(I) complex lacked the stretching vibration of the thiol (SH) group at 2562 cm^{-1}, indicating that the sulfur atom is coordinated to the metal center and the thione tautomer is more dominant than the thiol tautomer.[35] The strong band at 1458 cm^{-1} related to v(P-C) of the triphenylphosphine ligand.[36] The band at 457 cm^{-1} in the complex's IR spectrum may be attributed to C=S-Cu vibrations, whereas the band at 343 cm^{-1} is considered to be related to Cu-Cl vibrations.[37] Furthermore, the complex IR spectrum showed a high intensity band at 697 cm^{-1} corresponding to ν(Cu-P).[38]

3. 3. Electronic Spectra and Conductivity Study

The electronic absorption spectrum of the Cu (I) complex in dimethyl sulfoxide is dominated by two broad bands at 247 and 316 nm.[39] The first one is due to intra-ligand transitions of the triphenylphosphine ligand because uncoordinated triphenylphosphine shows a strong absorption band at 245 nm, which normally stays unshifted upon coordination to Cu(I).[40] The free 2-BIT ligand exhibits a band at 304 nm, whereas the absorption spectrum of the Cu(I) coordination complex is red-shifted by 12 nm, indicating C=S coordination to the Cu(I) center in the LMCT transition.[41] The molar conductivity value in DMSO (7.31×10^{-5} S cm^2 mol^{-1}) of the synthesized complex was found to be very low, suggesting that it is non-ionic in nature.[42]

3. 4. DFT Studies

The electronic characteristics of the ligands and Cu(I) complex were investigated using frontier molecular orbitals. The highest occupied molecular orbital (E_{HOMO}) and lowest unoccupied molecular orbital (E_{LUMO}) energies are used to calculate the HOMO-LUMO energy gap ($\Delta E = E_{LUMO} - E_{HOMO}$). The energy gaps of the ligands and Cu(I) complex are displayed in Table 4 and Figure 2. One of the most important theories for predicting complex reactivity and stability is the theory of frontier molecular orbitals. A reaction between two chemical compounds is shown by the interaction of one compound's HOMO orbital and another compound's LUMO orbital, according to this idea.[43] The energy gaps (ΔE) of the free 2-BIT and Ph_3P ligands are 6.573 eV and 6.706 eV, respectively, whereas the Cu(I) complex has an (ΔE) of 3.194 eV. Therefore, compared to ligands, the synthesized Cu(I) complex in our study is less stable and more reactive. The 2-BIT ligand appears to be less stable and more reactive than the triphenylphosphine ligand. Table 3 shows the computed NBO atomic charges for the free ligands and their complexes. The Natural Bond Orbitals (NBO) are used to compute electron densities (distributions) in atoms as well as bonds between atoms.[44]

The natural charges of the Cu atom reduce when 2-BIT is connected to Cu by its S atoms, which also become more positive (moved from 0.022e on the ligand alone to 0.226, 0.225e on the ligand coordinated to the Cu complex). However, the Cu-P complexes have changed slightly (from 0.842e to 0.977e and from 0.842 to 1.000e for P37 and P71), suggesting electron transfer from the Ph_3P ligand to the metal center.[45]

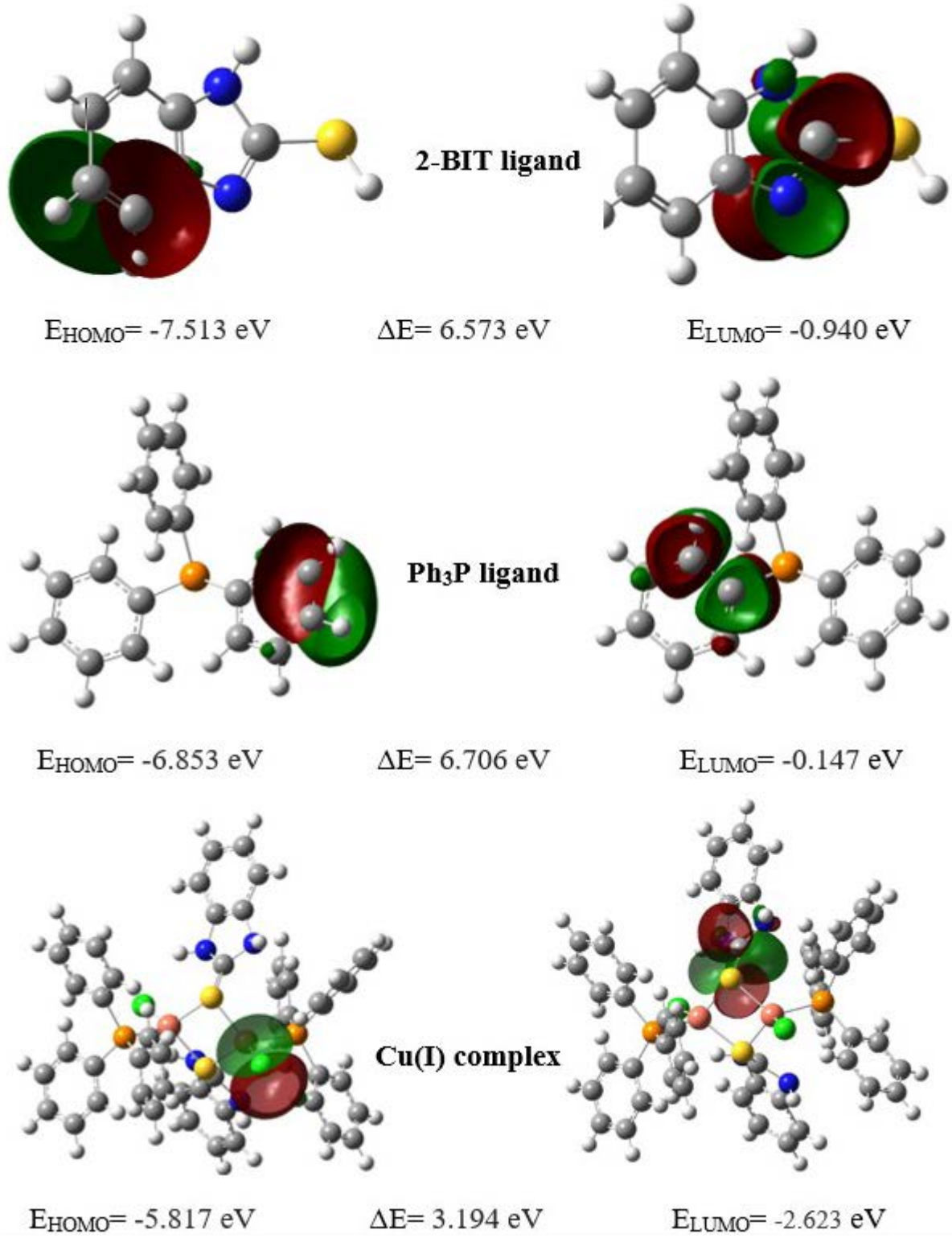

Figure 2. Surface plots of HOMO and LUMO orbitals of ligands and Cu(I) complex

Table 4. Energy properties (eV) and NBO Charge (e) of ligands and their Cu(I) complex.

Parameter	Ph_3P	2-BIT	Cu(I) complex
$_{EHOM}O$	–6.853	–7.513	–5.817
E_{LUMO}	–0.147	–0.940	*–2.623*
ΔE	6.706	6.573	3.194
The NBO Charge of ligands and Cu(I) complex			
Atom	**Ph_3P**	**2-BIT**	**Atom**	**Cu(I) complex**
N12	–	–0.480	Cu1, Cu2	–0.120, –0.166
N13	–	–0.580	S3, S4	0.226, 0.225
S	–	0.022	Cl5, Cl6	–0.553, –0.535
P	0.842	–	P37, P71	0.977, 1.000

3. 5. Hirshfeld Surfaces Analysis (HAS)

The Crystal Explorer 21.5 program was used to create the Hirshfeld surface analyses (HSA) and fingerprints of the Cu(I) complex.[46] The complex's fingerprint plots are shown in Figure 3. In a similar manner, Figure 4 displays the complex's Hirshfeld surface (HS). The d_{norm} surfaces are mapped in the range of –0.4424 to 1.5180 Å, while the shape index, and curvedness are mapped over ranges –1.0 to 1.0 Å, and –4.0 to 0.4 Å, respectively. The 2D fingerprint plots of the copper complex show that the major intermolecular interactions are H…H, H…C/C…H, H…Cl/Cl…H, C…C, and H…S/S…H as shown in Figure 4. The largest contribution to the overall Hirshfeld surface is due to H...H close contacts with 60.3%. The percentages of H…H, H…C/C…H, H…Cl/Cl…H, C…C, H…S/S…H, C…N/N…C, H…N/N…H, and Cl…C/C…Cl interactions are 60.3, 24.1, 7.0, 3.2, 3.1, 1.2, 1.0, and 0.1% of the complex surface, respectively. The d_{norm} surface detected very close intermolecular interactions, which were displayed as red spots and indicated short C–Cl…H, C–H…Cl, and C–C…H, C…H–C interactions. The stacking interaction can be investigated using the shape index and curvedness of HS, where blue areas represent convex regions of the compound inside the surface and red areas represent concave regions above the surface due to the π···π stacked complex's phenyl groups of triphenylphosphine and 2-benzimidazolethiole (L) ligands. Green flat areas on the curvedness surface also show the presence of π···π interaction in the Cu(I) complex.[47]

4. Conclusion

In conclusion, a new copper(I) complex was synthesized using triphenylphosphine and 2-benzimidazolethiole

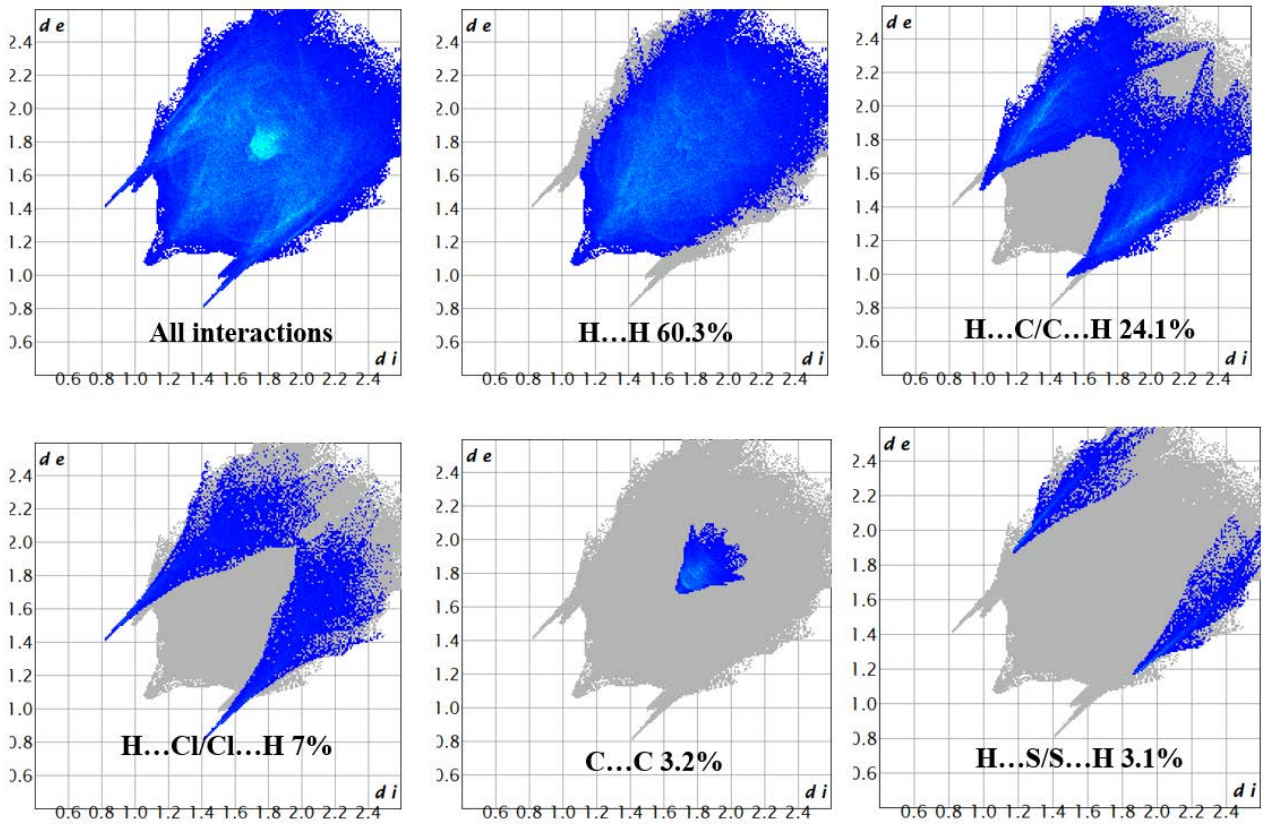

Figure 3. Fingerprint plots for the C(I) complex, showing percentages of major contact contributions to the total Hirshfeld surface analysis (HAS).

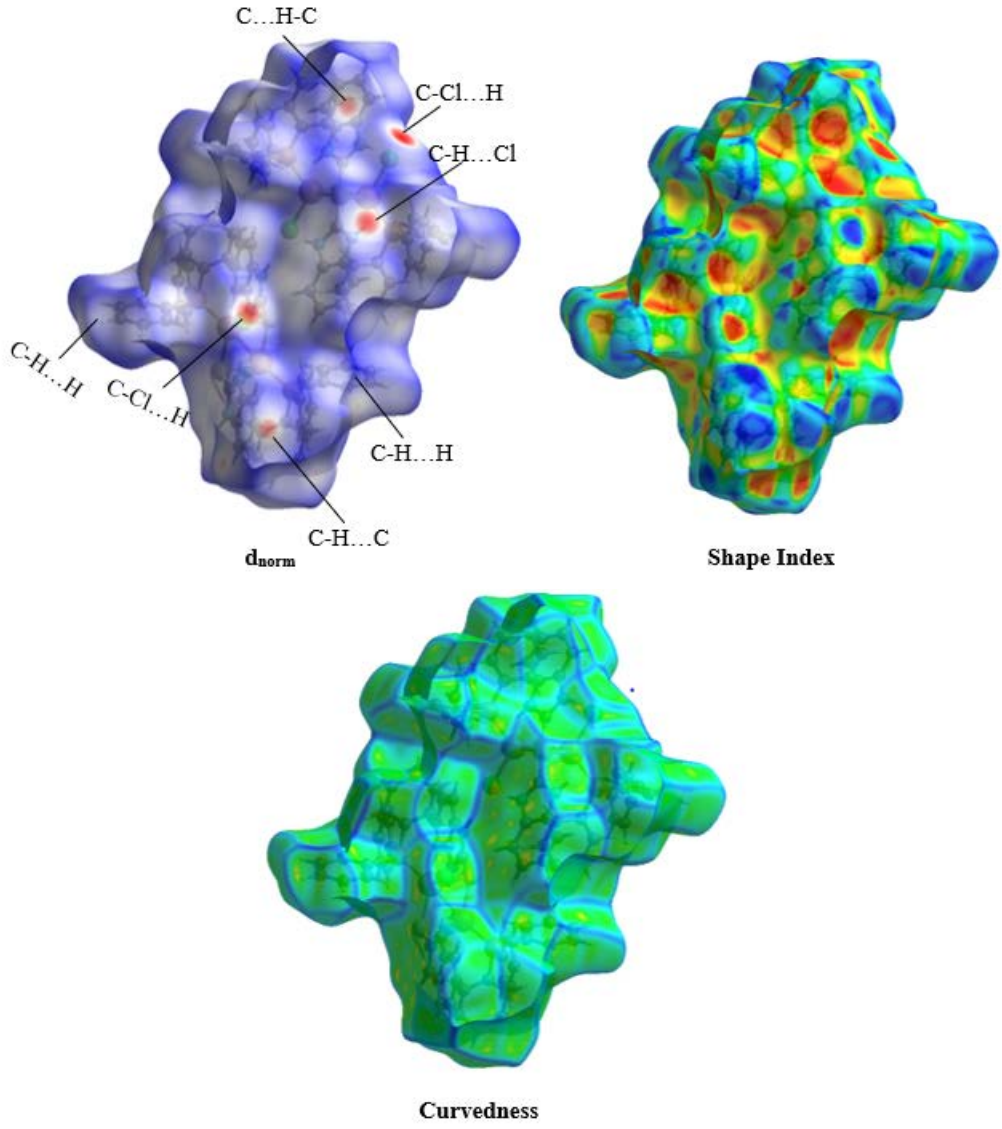

Figure 4. Hirshfeld surfaces mapped with *d*norm, shape index, and curvedness of the Cu(I) complex.

(L) ligands in a dichloromethane/methanol mixture. The spectroscopic techniques and X-ray crystallographic data revealed the synthesis of a binuclear copper complex with a 2-benzimidazolethiole ligand acting as a bridging ligand in thione form. The electronic spectrum of the complex displayed a peak at 31645 cm^{-1}, which corresponded to the ligand-to-metal charge transfer (LMCT) transition. The NBO analysis showed that the charge on the copper metals surrounded by the sulfur and phosphine atoms of the ligands (Cu1= –0.120 e, Cu2 = –0.166 e) is found to be less than the formal charge of the copper ion (+1) due to the transfer of electrons from the ligands to the metal center. According to the DFT study, the copper complex (ΔE= 3.194 eV) was less stable and more reactive than ligands. The Hirshfeld surface and 2D fingerprint plots analysis indicated that noncovalent interactions, such as H…H…H (60.3%), H…C/C…H (24.1%), and H…Cl/Cl…H (7%), constitute the driving force in stable crystal packing.

Supplementary material

Crystallographic data for the Copper(I) complex have been deposited with the Cambridge Crystallographic Data Center (CCDC), with the deposit number 1991210. The data can be obtained free of charge at http://www.ccdc.cam.ac.uk/conts/retrieving.html.

Acknowledgments

The authors gratefully acknowledge access to the X-ray facilities at Nelson Mandela University, Port Elizabeth, South Africa. We also thank Mr. Mzgin Ayoob for his FT-IR instrumental support.

Funding

The author would like to acknowledge the college of science at the University of Halabja in Kurdistan Region, Iraq, for providing the financial funding for this study.

5. References

1. R. Czerwieniec, M. J. Leitl, H. H. Homeier, H. Yersin, *Coord. Chem. Rev*. **2016**, *325*, 2–28. **DOI:**10.1016/j.ccr.2016.06.016
2. B. A. Babgi, *J. Organomet. Chem*. **2021**, *956*, 122124. **DOI:**10.1016/j.jorganchem.2021.122124
3. A. Kobayashi, M. Kato, *Chem. Lett*. **2017**, *46*, 154–162. **DOI:**10.1246/cl.160794
4. H. A. Mohamad, K. O. Ali, E. Hosten, T. Gerber, *Chinese J. Inorg. Chem*. **2021**, *37*, 1106–1112. **DOI:**10.51380/gujr-37-02-01
5. H. S. Seleem, B. A. El-Shetary, M. Shebl, *Heteroat. Chem*. **2007**, *18*, 100–107. **DOI:**10.1002/hc.20239
6. A. K. El-Sawaf, F. El-Essawy, A. A. Nassar, E. A. El-Samanody, *J. Mol. Struct*. **2018**, *1157*, 381–394. **DOI:**10.1016/j.molstruc.2017.12.075
7. O. M. Adly, H. F. El-Shafiy, M. Shebl. *J. Mol. Struct*. **2019**, *1196*, 805–818. **DOI:**10.1016/j.molstruc.2019.07.010
8. A. Fetoh, M. A. Mohammed, M. M. Youssef, G. M. Abu El-Reash, *J. Mol. Liq*. **2019**, *287*, 110958. **DOI:**10.1016/j.molliq.2019.110958
9. M. Shebl, *J. Mol. Struct*. **2017**, *1128*, 79–93. **DOI:**10.1016/j.molstruc.2016.08.056
10. A. Y. Lukmantara, D. S. Kalinowski, N. Kumar, D. R. Richardson, *J. Inorg. Biochem*. **2014**, *141*, 43–54. **DOI:**10.1016/j.jinorgbio.2014.07.020
11. M. Z. M. Zubir, N. S. Jamaludin, S. N. A. Halim, *J. Mol. Struct*. **2019**, *1193*, 141–150. **DOI:**10.1016/j.molstruc.2019.05.011
12. D. Anastasiadou, G. Psomas, M. Lalia-Kantouri, A. G. Hatzidimitriou, P. Aslanidis, *Mater. Sci. Eng. C*. **2016**, *68*, 241–250. **DOI:**10.1016/j.msec.2016.05.112
13. I. I. Ozturk, E. T. Sirinkaya, M. Cakmak, M. Gürgan, D. Ceyhan, N. Panagiotou, A. J. Tasiopoulos, *J. Mol. Struct*. **2021**, *1227*, 129730. **DOI:**10.1016/j.molstruc.2020.129730
14. A. Singh, M. Trivedi, G. Kociok-Köhn, A. K. Singh, M. Muddassir, A. Kumar, *Cryst. Eng. Comm*. **2021**, *23*, 7794–7804. **DOI:**10.1039/D1CE01147B
15. F. Karasmani, A. Tsipis, P. Angaridis, A. G. Hatzidimitriou, P. Aslanidis, *Inorganica Chim. Acta*. **2018**, *471*, 680–690. **DOI:**10.1016/j.ica.2017.12.002
16. H. F. Abd El-Halim, G. G. Mohamed, M. N. Anwar, *Appl. Organometal. Chem*. **2018**, *32*, e3899. **DOI:**10.1002/aoc.3899
17. M. Shebl, S. M. Khalil, A. Taha, M. A. N. Mahdi, *J. Mol. Struct*. **2012**, *1027*, 140–149. **DOI:**10.1016/j.molstruc.2012.05.067
18. O. M. I. Adly, M. Shebl, E. M. Abdelrhman, B. A. El-Shetary, *J. Mol. Struct*. **2020**, *1219*, 128607. **DOI:**10.1016/j.molstruc.2020.128607
19. S. L. Liu, C. L. Wen, S. S. Qi, E. X. Liang, *Spectrochim. Acta A Mol. Biomol. Spectrosc.* **2008**, *69*, 664–669. **DOI:**10.1016/j.saa.2007.05.019
20. M. Shebl, O. M. Adly, A. Taha, N. N. Elabd, *J. Mol. Struct*. **2017**, *1147*, 438–451. **DOI:**10.1016/j.molstruc.2017.06.085
21. S. L. Liu, C. L. Wen, C. Chen, S. S. Qi, E. X. Liang, *Mater. Res. Bull*. **2008**, *43*, 2397–2402. **DOI:**10.1016/j.materresbull.2007.07.040
22. N. Nabil, O. M. I. Adly, M. Shebl, A. Taha, F. Samy, *RSC Adv*. **2022**, *12*, 29939–29958. **DOI:**10.1039/D2RA03475A
23. R. Neelaeni, S. Vasantha, R. Keerthana, S. Sivakolunthu, T. Angeline, *Asian J. Pharm. Clin. Res*. **2016**, *9*, 277–281.
24. G. M. Sheldrick, *Acta Cryst. A*. **2015**, *71*, 3–8. **DOI:**10.1107/S2053229614024218
25. C. B. Hübschle, G. M. Sheldrick, B. Dittrich, *J. Appl. Crystallogr*. **2011**, *44*, 1281–1284. **DOI:**10.1107/S0021889811043202
26. L. Krause, R. Herbst-Irmer, G. M. Sheldrick, D. Stalke, *J. appl. Cryst*. **2015**, *48*, 3–10. **DOI:**10.1107/S1600576714022985
27. I. Rajaei, S. N. Mirsattari, *Polyhedron*. **2015**, *102*, 479–489. **DOI:**10.1016/j.poly.2015.10.019
28. B. Rajasekhar, N. Patowary, D. KZ, T. Swu, *Mol. Phys*. **2018**, *116*, 1883–1894. **DOI:**10.1080/00268976.2018.1460497
29. S. L. Chen, Z. Liu, J. Liu, G. C. Han, Y. H. Li, *J. Mol. Struct*. **2012**, *1014*, 110–118. **DOI:**10.1016/j.molstruc.2012.02.011
30. M. Ikram, S. Rehman, I. Feroz, R. Khan, M. O. Sinnokrot, F. Subhan, M. Naeem, C. Schulzke, *Mol. Struct*. **2023**, *1278*, 134960. **DOI:**10.1016/j.molstruc.2023.134960
31. J. Mondal, A. K. Manna, G. K. Patra, *Eur. J. Chem*. **2020**, *11*, 334–341. **DOI:**10.5155/eurjchem.11.4.334-341.2037
32. P. J. Cox, P. Aslanidis, P. Karagiannidis, *Polyhedron*. **2000**, *19*, 1615–1620. **DOI:**10.1016/S0277-5387(00)00438-1
33. V. P. Singh, P. Singh, A. K. Singh, *Inorg. Chim. Acta*. **2011**, *379*, 56–63. **DOI:**10.1016/j.ica.2011.09.037
34. L. H. Wang, X. Y. Qiu, S. J. Liu, *Acta Chim. Slov*. **2019**, *66*, 675–680. **DOI:**10.17344/acsi.2019.5117
35. L. A. Mohammed, N. I. Mahdi, R. A. B. Aldujaili, *Egypt. J. Chem*. **2020**, *63*, 289–300. **DOI:**10.21608/ejchem.2019.19821.2195
36. S. S. Devkule, S. S. Chavan, *Inorganica Chim. Acta*. **2017**, *466*, 122–129. **DOI:**10.1016/j.ica.2017.05.076
37. P. Tyagi, S. Chandra, B. S. Saraswat, D. Yadav, *Spectrochim. Acta – A: Mol. Biomol. Spectrosc*. **2015**, *145*, 155–164. **DOI:**10.1016/j.saa.2015.03.034
38. T. Bal-Demirci, Ş. Güveli, S. Yeşilyurt, N. Özdemir, B. Ülküseven, *Inorganica Chim. Acta*. **2020**, *502*, 119335. **DOI:**10.1016/j.ica.2019.119335
39. L. H. Wang, X. Y. Qiu, S. J. Liu, *J. Coord. Chem*. **2019**, *72*, 962–971. **DOI:**10.1080/00958972.2019.1590561
40. S. M. Khalil, M. Shebl, F. S. Al-Gohani, *Acta Chim. Slov*. **2010**, *57*, 716–725.
41. K. J. Koebke, L. Ruckthong, J. L. Meagher, E. Mathieu, J. Harland, A. Deb, N. Lehnert, C. Policar, C. Tard, J. E. Penner-Hahn, J. A. Stuckey, *Inorg. Chem*. **2018**, *57*, 12291–12302. **DOI:**10.1021/acs.inorgchem.8b01989
42. P. Singh, D. P. Singh, K. Tiwari, M. Mishra, A. K. Singh, V. P. Singh, *RSC Adv.* **2015**, *5*, 45217–45230. **DOI:**10.1080/24701556.2020.1770794 **DOI:**10.1039/C4RA11929K
43. M. Shebl, A. A. Saleh, S. M. Khalil, M. Dawy, A. A. Ali, *Inorg. Nano-Met. Chem*. **2021**, *51*, 195–209.
44. L. Saghatforoush, K. Moeini, S. A. Hosseini-Yazdi, Z. Mardani, A. Bakhtiari, A. Hajabbas-Farshchi, S. Honarvar, M. S. Abdelbaky, *Polyhedron*. **2019**, *170*, 312–324. **DOI:**10.1016/j.poly.2019.05.057
45. L. Saghatforoush, K. Moeini, S. A. Hosseini-Yazdi, Z. Mardani, A. Hajabbas-Farshchi, H. T. Jameson, S. G. Telfer, J. D. Woollins, RSC adv. **2018**, *8*, 35625–35639. **DOI:**10.1039/C8RA07463A

46. E. Alaman, A. A. Ağar, M. N. Tahir, M. Ashfaq, E. B. Poyraz, N. Dege, *J. Struct. Chem.* **2023**, *64*, 1314–1328. **DOI:**10.1134/S0022476623070156

47. Y. Zhang, Y. Q. Pan, M. Yu, X. Xu, W. K. Dong, *Appl. Organomet. Chem.* **2019**, *33*, e5240. **DOI:**10.1002/aoc.5368

Povzetek

Z reakcijo med 2-benzimidazoltiolom (L) in bakrovim dikloridom v prisotnosti dvakratne množine trifenilfosfina smo sintetizirali nov dvojedrni kompleks $[Cu(L)_2(Ph_3P)_2Cl_2]$: dikloridobis(μ-1,3-dihidro-2H-benzimidazol-2-tion) bis(trifenilfosfin)-di-baker. Spojino bakra(I) smo karakterizirali z elementno analizo, meritvami molske prevodnosti, FT-IR, UV/Vis in monokristalno rentgensko difrakcijo. Strukturna analiza je pokazala, da ima kompleks popačeno tetraedrično geometrijo okoli centralnega Cu(I), z dvema mostovnima atomoma žvepla. Hirschfeldova površinska analiza na d_{norm} je pokazala, da so medmolekulske interakcije H…H, H…C/C…H in H…Cl/Cl…H ključne za pakiranje kristalov. Za razumevanje nukleofilnih in elektrofilnih interakcij med ligandom in Cu(I) ioni smo uporabili naravno vezno orbital (NBO). Za prikaz molekularne reaktivnosti oziroma stabilnosti ligandov in kompleksa smo uporabili izračune DFT.